CrossMark

ORIGINAL PAPER

Nanoparticulate Tetrac Inhibits Growth and Vascularity of Glioblastoma Xenografts

Thangirala Sudha[1] · Dhruba J. Bharali[1] · Stewart Sell[2] · Noureldien H. E. Darwish[1,3] ·
Paul J. Davis[1,4,5] · Shaker A. Mousa[1,5]

Abstract Thyroid hormone as L-thyroxine (T_4) stimulates proliferation of glioma cells in vitro and medical induction of hypothyroidism slows clinical growth of glioblastoma multiforme (GBM). The proliferative action of T_4 on glioma cells is initiated nongenomically at a cell surface receptor for thyroid hormone on the extracellular domain of integrin $\alpha v \beta 3$. Tetraiodothyroacetic acid (tetrac) is a thyroid hormone derivative that blocks T_4 action at $\alpha v \beta 3$ and has anticancer and anti-angiogenic activity. Tetrac has been covalently bonded via a linker to a nanoparticle (Nanotetrac, Nano-diamino-tetrac, NDAT) that increases the potency of tetrac and broadens the anticancer properties of the drug. In the present studies of human GBM xenografts in immunodeficient mice, NDAT administered daily for 10 days subcutaneously as 1 mg tetrac equivalent/kg reduced tumor xenograft weight at animal sacrifice by 50%, compared to untreated control lesions ($p < 0.01$). Histopathological analysis of tumors revealed a 95% loss of the vascularity of treated tumors compared to controls at 10 days ($p < 0.001$), without intratumoral hemorrhage. Up to 80% of tumor cells were necrotic in various microscopic fields ($p < 0.001$ vs. control tumors), an effect attributable to devascularization. There was substantial evidence of apoptosis in other fields ($p < 0.001$ vs. control tumors). Induction of apoptosis in cancer cells is a well-described quality of NDAT. In summary, systemic NDAT has been shown to be effective by multiple mechanisms in treatment of GBM xenografts.

✉ Paul J. Davis
    pdavis.ordwayst@gmail.com

[1] Pharmaceutical Research Institute, Albany College of Pharmacy and Health Sciences, 1 Discovery Drive, Rensselaer, NY 12144, USA

[2] Wadsworth Center, New York State Department of Health, Albany, NY, USA

[3] Department of Clinical Pathology, Faculty of Medicine, Mansoura University, Mansoura, Egypt

[4] Department of Medicine, Albany Medical College, Albany, NY, USA

[5] NanoPharmaceuticals LLC, Rensselaer, NY, USA

Introduction

Glioblastoma multiforme (GBM) is an aggressive central nervous system tumor with high mortality [1, 2]. The tumor is also relatively chemoresistant [3, 4] and radioresistant [5]. Its invasiveness and asymmetry result in fewer than 30% of patients at presentation having tumors amenable to total resection [6]. The cancer is highly vascular, causing the evaluation of anti-angiogenesis in its management [7]. Against this background, it is understandable that a number of novel therapeutic approaches are under investigation [8–10].

Hercbergs and co-workers in a prospective, controlled clinical study developed evidence that GBM is thyroid hormone dependent, that is, medical induction of mild hypothyroidism slowed the course of the disease [11]. We reported that thyroid hormone, L-thyroxine (T_4), was a proliferative factor in vitro in rat C6 and F98 cells and mouse GL261 cell line models for glioblastoma [12]. This effect was mediated by the cell surface thyroid hormone receptor we described on plasma membrane integrin $\alpha v \beta 3$ [13, 14]. The deaminated T_4 derivative, tetraiodothyroacetic acid (tetrac), blocked the proliferative action nongenomically initiated by T_4 on these cells [12].

We also demonstrated that thyroid hormone was anti-apoptotic in glioma cells [15]. In studies of a human GBM cell line (U87MG), we defined discrete domains in the thyroid hormone receptor on $\alpha v\beta 3$ that bound T_3 and both T_4 and T_3 [16]. The T_3 domain activated phosphatidylinositol 3-kinase (PI3-K), whereas mitogen-activated protein kinase (MAPK; ERK1/2) signal transduction pathway was activated by the T_4/T_3 domain. The latter supported U87MG cell proliferation.

We subsequently showed in a variety of xenografts that a formulation of tetrac covalently linked to a nanoparticle (Nanotetrac, Nano-diamino-tetrac, NDAT)—an agent thus restricted to the extracellular space and to action at the integrin—effectively slowed tumor growth and reduced vascularity [17–21]. The nanoparticle in this agent is biodegradable poly (lactic-co-glycolic acid) (PLGA). The antitumor effectiveness of NDAT involves pro-apoptotic activity and disruption of transcription of genes essential to a number of cancer cell survival pathways. The anti-angiogenic activity of NDAT involves disordering by several mechanisms of actions of endogenous growth factors, such as vascular endothelial growth factor (VEGF) [22], basic fibroblast growth factor (bFGF; FGF2) [22] and platelet-derived growth factor (PDGF) (S.A. Mousa, unpublished observations). NDAT also downregulates expression of the epidermal growth factor receptor (EGFR) gene [23]. Again, all of these actions are nongenomically initiated at integrin $\alpha v\beta 3$.

In the present studies, we document the efficacy of systemic NDAT, acting via the thyroid hormone-tetrac receptor on integrin $\alpha v\beta 3$ against human U87MG glioblastoma xenografts.

Materials and Methods

Cultured U87MG-luc Cells Human glioblastoma U87MG-luc cells were a generous gift from MD Anderson Cancer Center, Houston, TX, and were grown in DMEM supplemented with 10% fetal bovine serum, 1% penicillin, and 1% streptomycin. Cells were cultured at 37 °C to sub-confluence and treated with 0.25% (w/v) trypsin/EDTA to effect cell release from culture flask. Cells were washed with culture medium, suspended in DMEM that was free of phenol red and fetal bovine serum, and counted. Medium and other culture materials were from Sigma-Aldrich (St. Louis, MO).

Animals Immunodeficient, female NCr nude homozygous mice aged 5–6 weeks and weighing between 18 and 20 g were purchased from Envigo (Indianapolis, IN). All animal studies were conducted at the animal facility of the Veteran Affairs Medical Center, Albany, NY, in accordance with and approved by institutional guidelines for humane animal treatment and according to the current guidelines. Mice were maintained under specific pathogen-free conditions and housed under controlled conditions of temperature (20–24 °C) and humidity (60–70%) and 12-h light/dark cycle with ad libitum access to water and food. Mice were allowed to acclimatize for 5 days prior to the start of study.

Tetrac, NDAT Tetrac was obtained from KareBay Biochem, Inc. (Monmouth Junction, NJ) and solubilized as previously described [19, 20], and NDAT was generated as previously described [19]. Both chemical structures are shown in the Supplemental Data. The nanoparticle diameter distribution, morphology, and zeta potential have also been reported [24]. The product consists of tetrac that is ether-bonded to a diaminoproprane linker via the outer ring hydroxyl group of tetrac. The linker is then attached by an amide bond to a nanoparticle of PLGA of approximately 150–200 nm. The agent is administered subcutaneously (s.c.) as a suspension in PBS. The amount of tetrac, itself, that is administered in NDAT is corrected for the contributions to molecular weight of the linker and PLGA nanoparticle.

Treatment In the first set of experiments, there were two discrete xenografts/animal and four animals in each of six experimental groups (control, void nanoparticle, tetrac (3 μg), tetrac (10 μg), NDAT (3 μg), NDAT (10 μg)). Cancer cells (2×10^6), together with the respective control or treatment compound, were implanted s.c. in each flank of each animal. The control was PBS, and treatment compounds were void nanoparticle (volume = 10 μg NDAT dose), unmodified tetrac (3 or 10 μg), or NDAT (3 or 10 μg). NDAT at 10 μg/implant achieves an intratumoral tetrac equivalent concentration of approximately 10^{-7} M [25]. After humane sacrifice of animals at 16 days, tumors were harvested and hemoglobin concentration determined (see method below) to estimate graft vascularity. Tumor cell viability was estimated with In Vivo Imaging System (IVIS) scanning (see method, below).

In the second set of experiments, there were two grafts/animal and four animals for each experimental condition (control, NDAT). Xenografts consisted of 2×10^6 cancer cells implanted s.c. in each flank of each mouse. After 2 days, the animals were treated daily with control (PBS) or NDAT (1 mg/kg) s.c. for 10 days. Animals were then humanely sacrificed and harvested tumors were subjected to histopathology examination.

Estimation of Hemoglobin Content Graft vascularity in the harvested tumors was estimated from an angiogenesis index of tumor cell lysate (tumor hemoglobin, mg/dL) measured with Drabkin's reagent (Sigma-Aldrich) and with a hemoglobin standard, as described previously [21].

Estimation of Tumor Cells' Viability Viability of cells in situ in harvested tumors from U87MG-luc cell-grafted animals

was determined with luminescent signal measurement in an IVIS® apparatus (PerkinElmer Inc., Waltham, MA).

Histopathology Histopathology assessment of morphologic evidence of cell necrosis and apoptosis was done for slides prepared from the harvested tumors. Harvested xenografts were fixed in formalin, embedded in paraffin, and sectioned at the Wadsworth Center Core Histology Laboratory, New York State Department of Health. Paraffin-embedded tissue sections were stained with hematoxylin and eosin (H&E). Each tissue section was coded and examined by a board-certified pathologist who had no knowledge of the treatment exposure of the tissue (= blinded interpretation). The area of the tissue section was measured with a stage micrometer and the percentage of viable vs. necrotic tumor was estimated visually. The number of mitoses and apoptotic cells per high-power field was counted for five fields of viable tumor areas and averaged per tissue section. The degree of vascularization varied in the viable areas and this was graded numerically 1 to 4.

Estimation of Tumor Volume and Weight Tumor width and length were estimated with calipers at 3-day intervals and volume calculated from the standard formula ($W \times L^2/2$). Tumor weight was measured in harvested lesions following humane sacrifice of animals.

Statistics Statistical analysis was performed using one-way ANOVA, comparing the mean ± SEM from each experimental group with its relevant control group. Statistical differences at $p < 0.05$ were considered significant.

Results

Effect of Tetrac/NDAT Injected Intratumorally at Time of Implant on GBM Xenografts

Tumor Weight At animal sacrifice after day 16, harvested tumor weights were measured. Tetrac at 10 μg and NDAT at both 3 and 10 μg reduced tumor weight significantly compared to control tumors, *$p < 0.01$ (Fig. 1a).

Hemoglobin Assay For a measurement of tumor vascularity, the hemoglobin content of cell extracts of xenografts revealed that NDAT treatment resulted in a 50% loss of tumor blood vessel content (Fig. 1b).

Cell Viability IVIS scanning of excised U87MG-luc xenografts revealed virtually complete loss of viability of cells in the NDAT (10 μg) and substantial reduction in viability in grafts treated with 3 μg NDAT and 10 μg unmodified tetrac (Fig. 2a). Tetrac at 3 μg was ineffective. Figure 2b is the quantitative analysis of bioluminescence results depicted in Fig. 2a and shows an 80% reduction in cell viability with NDAT at 3 μg and with tetrac at 10 μg. NDAT at 10 μg completely eliminated tumor cell viability.

Effect of Tetrac/NDAT Administered s.c. Daily on Established GBM Xenografts

Tumor Weight and Volume At animal sacrifice after 10 days of treatment with NDAT, estimated volumes of harvested tumors decreased by 60%, compared to controls (Fig. 3a). In agreement with this measurement, there was a reduction in harvested tumor weight of 50% (*$p < 0.01$), compared to

Fig. 1 Effects at 16 days after single injection of U87MG cancer cells along with various treatments. There were four animals per group and two tumors per animal, n = 8. *Error bars* represent ±SEM and statistical significance is compared to control, *$p < 0.01$. **a** Tumor weights for control (PBS), void nanoparticle (NP), tetrac (3 μg), tetrac (10 μg), NDAT (3 μg), and NDAT (10 μg). **b** Hemoglobin content for the same groups
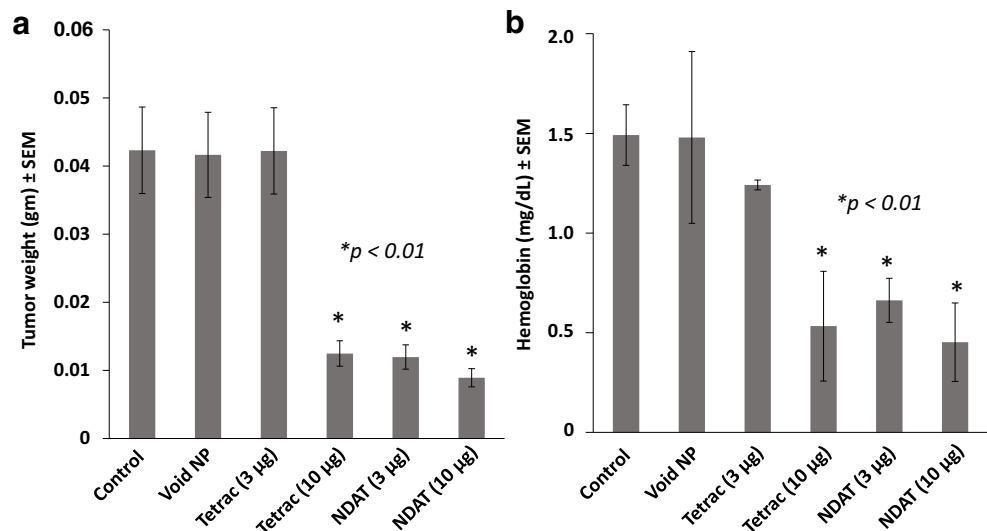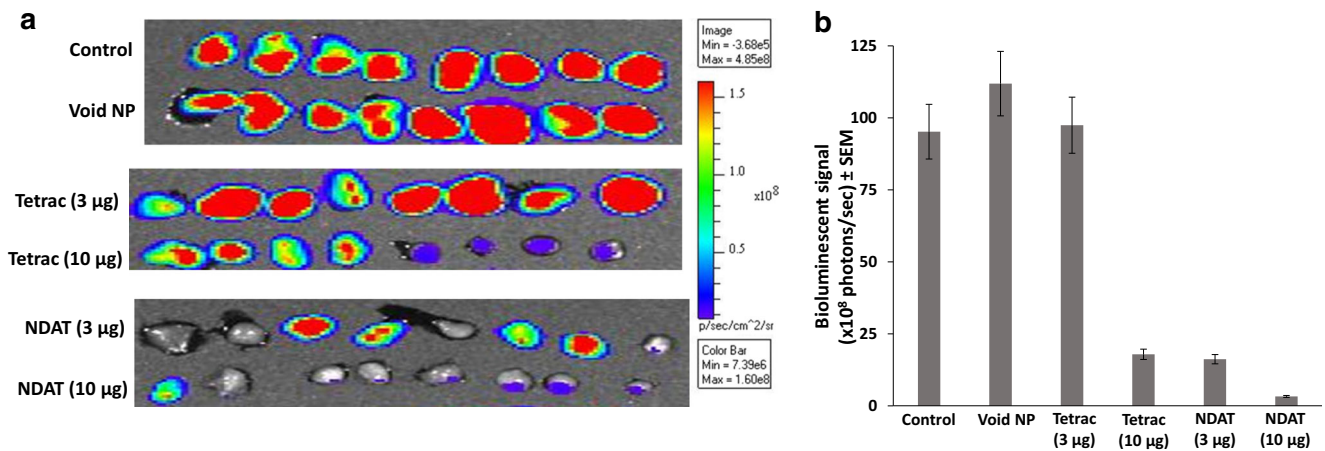
Fig. 2 IVIS imaging of harvested tumors 16 days after single injections of U87MG-luc cancer cells along with various treatments; there were four animals per group and two tumors per animal. **a** Effects of control (PBS), void nanoparticle (NP), tetrac (3 μg), tetrac (10 μg), NDAT (3 μg), and NDAT (10 μg). The *vertical luminescence color bar* (*right side*) estimates viability, ranging from nonviable (*blue*) to fully viable (*red*). NDAT at 10 μg/implant approximates 10^{-7} M tissue tetrac equivalent drug concentration. **b** Quantitation of the tumor bioluminescent signal intensity in **a**. *Error bars* represent ±SEM compared to control, $n = 8$

control tumors (Fig. 3b). We note that three of the four control animals died on day 9, and their tumors' volume and weight reflect 9 days of treatment.

Histopathology Figure 4a–c shows necrosis at low magnification of control (a) and NDAT-treated tumors (b–c). There is extensive necrosis on histologic evaluations of U87MG tumors harvested at 10 days from NDAT-treated animals. That is, in tumors from NDAT-treated mice, there was loss of tissue/cell density and of nuclear structure, as well as dissolution of plasma membrane. Shown quantitatively in Fig. 5,

such necrotic changes were present in many slide fields in up to 80% of tumor cells from treated animals (**$p < 0.001$ vs. control tumors). Estimated cell density in tumors exposed to NDAT was reduced by 60%, compared to controls (**$p < 0.001$). Percentages reported in these histologic interpretations are means of observations made on multiple fields of four slides of each xenograft. Figure 5 also indicates that regions were frequently identified in NDAT-treated tumors in which apoptotic changes were prominent in cancer cells. In such regions, 40% of cells were apoptotic (**$p < 0.001$ vs. untreated tumors). Such evidence includes cell shrinkage,

Fig. 3 Effect of 10 days of daily s.c. NDAT (1 mg/kg) treatment on U87MG glioblastoma xenograft volume and weight. There were four animals per group and two tumors per animal, $n = 8$. *Error bars* represent ±SEM and statistical significance is compared to control. Three of the four control animals died on day 9, and their tumors' volume and weight reflect 9 days of treatment. **a** Volumes of harvested tumors decreased by 60%, compared to controls. **b** There was a reduction in harvested tumor weight of 50% (*$p < 0.01$), compared to control lesions
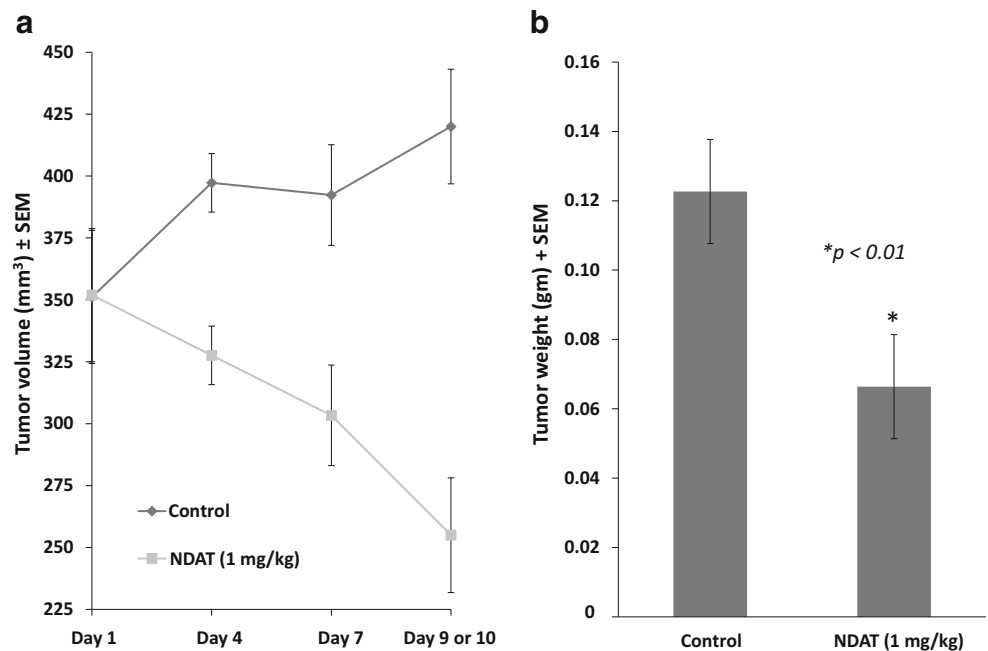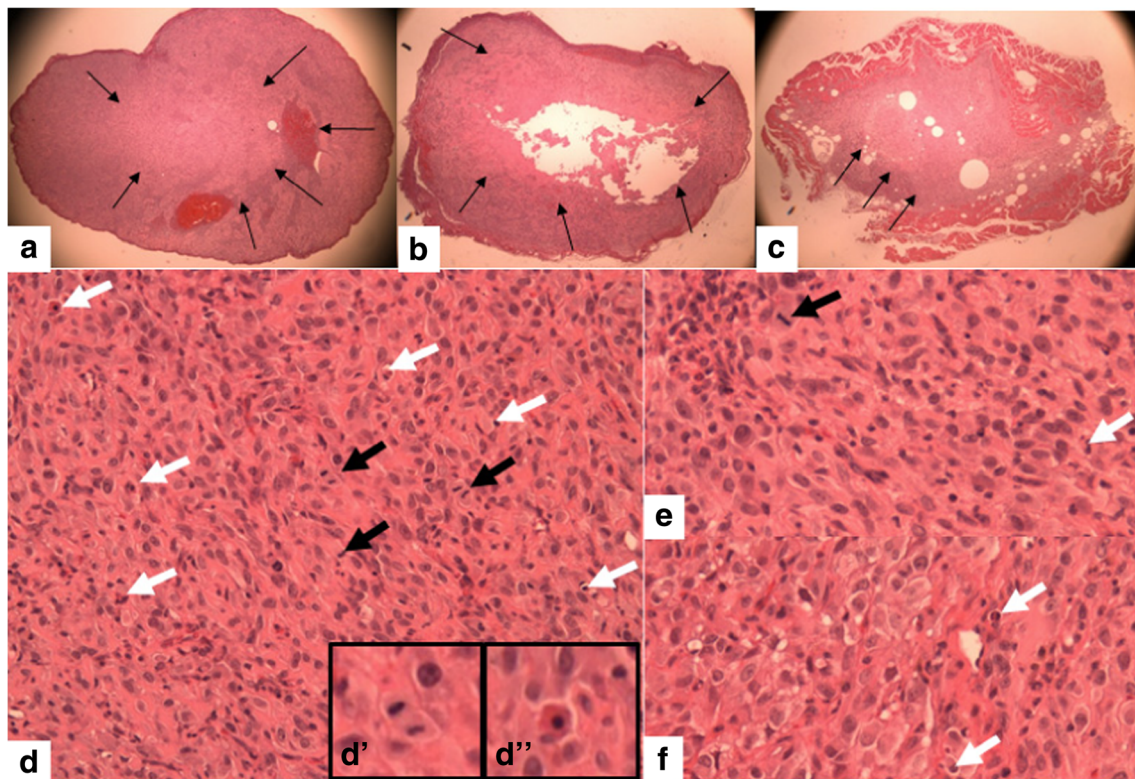
Fig. 4 Histology showing effect of 10 days of daily s.c. NDAT treatment (1 mg/kg) on U87MG glioblastoma xenografts. **a–c**: Low power views of histologic sections of tumor xenografts harvested from control and NDAT-treated animals. **a** Sections from untreated animal, showing decreased cellularity in central area of tumor (*small arrows*), but not complete necrosis. **b, c** Sections from tumors of treated animals reveal extensive central necrosis involving 50% of tumor mass (**b**) or a smaller tumor (**c**) containing less than 30% viable cells. *Small arrows* show border of viable cells, and in **b**, part of the central necrotic area has been lost during processing of the tissue. *Lower 3 panels* (**d–f**) are high-power (400×) views of sections from tumors of NDAT-treated animals, showing cells undergoing necrosis (*black arrows*) and apoptosis (*white arrows*). *Insets D′ and D″* show mitosis and apoptosis, respectively. Apoptotic cells have pyknotic nuclei and condensed eosinophilic cytoplasm and show separation from adjacent viable cells. In necrotic areas, there is no cellular morphology or nuclear staining

patchy condensation of nuclear chromatin, and increased density of cytoplasm. Figure 5 indicates that essentially all of the vascularity of NDAT-exposed tumors had disappeared (**p < 0.001 vs. control tumors). Figure 6a shows that tumor areas in histologic cross-sections of excised whole xenografts were reduced by 80% in animals receiving NDAT daily × 10 days, compared to control (**p < 0.001). The number of mitotic cells/microscopic field was decreased by 77% in xenografts of NDAT-treated animals compared to control (**p < 0.001).

There were no examples of intratumoral hemorrhage in xenografts from drug-treated or control animals, and animal weights over the 10-day treatment period were unaffected by NDAT administration (data not shown).

Discussion

A variety of chemotherapeutic [26–28] and anti-angiogenic [29] approaches have been used to manage GBM clinically. Success has been limited and a number of new chemotherapeutic and immunotherapeutic strategies are under development [30–34]. Further, the introduction of treatment agents directly by a catheter into tumors [35–38] offers the prospect of achieving high local concentrations of drug, bypass of the blood-brain barrier—although the latter may be porous about tumors [39, 40]—and limitation of systemic drug toxicity. Because of inherent radioresistance of this tumor, agents that radiosensitize are also of particular interest in management of glioblastoma.

In the present study, we determined the effectiveness of systemic NDAT (Nanotetrac, Nano-diamino-tetrac) against glioblastoma cell xenografts. The agent reduced tumor size promptly, effectively devascularized the tumors, and induced necrosis—presumably reflecting the loss of graft vascular supply—and apoptosis in cells not undergoing necrosis. Consistent with these findings, cell density in tumors from treated animals was reduced. In contrast to actions of other anti-angiogenic drugs tested oncologically [41–43], NDAT did not induce hemorrhage in the tumors or hemorrhagic events elsewhere. The basis of this finding in NDAT-exposed animals is not clear, but we propose that the effects on angiogenesis regulated from integrin αvβ3 can include systematic takedown of
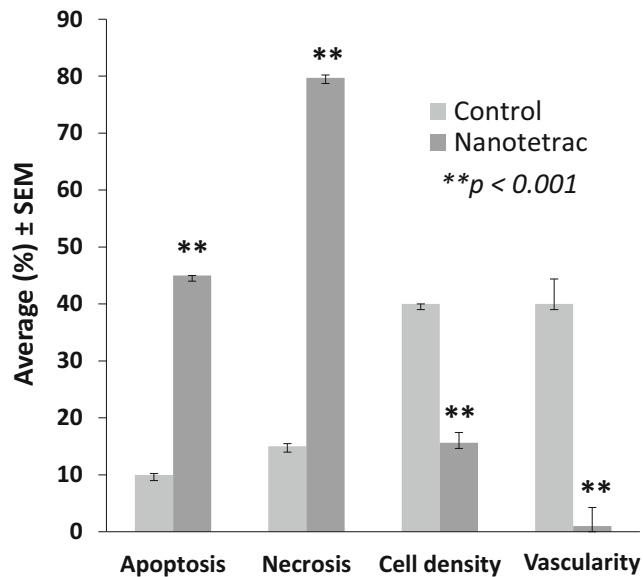
Fig. 5 Induction of necrosis by 10 days of daily s.c. NDAT treatment (1 mg/kg) in U87MG glioblastoma xenografts significantly increased necrosis and apoptosis in various fields. As a result, cell density was reduced. The vasculature essentially disappeared from xenografts of NDAT-treated animals. Data were collected from four animals per group and two tumors per animal, $n = 8$. *Error bars* represent ±SEM and statistical significance is compared to control, **$p < 0.001$

its target/receptor on $\alpha v \beta 3$ the transcription of a number of genes important to regulation of cell division [23, 44, 45].

In earlier in vitro studies, we showed that three rodent glioma cell lines proliferated in response to thyroid hormone and that this proliferative effect was blocked by tetrac [12]. T_3 and T_4 were equipotent in these experiments, but free T_4 concentrations in human subjects are 50-fold those of free T_3, so that the responsiveness of GBM to thyroid hormone, dictated by the hormone receptor site on integrin $\alpha v \beta 3$, is T_4 based. NDAT inhibits binding of T_4 and T_3 to the integrin as one mechanism of antitumor action, but NDAT has a number of antitumor properties that are independent of agonist thyroid hormone, as was pointed out above. In addition to rodent glioma studies, we have also reported that a human GBM cell line (U87MG) proliferates when thyroid hormone is added to the medium in amounts that produce a directly measured physiologic level of free hormone [16]. This hormonal action is mediated by mitogen-activated protein kinase (MAPK; ERK1/2).

Beyond anti-proliferation at the level of the tumor cell, a second important facet of the properties of NDAT is that it is anti-angiogenic by multiple mechanisms [14]. This should be particularly relevant to GBM because of its extensive vascularity. NDAT inhibits actions of vascular endothelial growth factor (VEGF) [22, 46], basic fibroblast growth factor (bFGF) [47], platelet-derived growth factor (PDGF) (S.A. Mousa, unpublished observations), and epidermal growth factor (EGF) [48]. Depending on the growth factor, these effects can involve gene transcription, growth factor release, or inhibitory crosstalk between the thyroid hormone-tetrac receptor on integrin $\alpha v \beta 3$ and the vascular growth factor receptors clustered with the integrin on or in the plasma membrane.

A third facet of NDAT actions is that the agent increases radiosensitivity of human glioblastoma cells in vitro [49]. This

vasculature and not only inhibition of new blood vessel formation.

Cell necrosis in the context of devascularized tumors was expected. That apoptosis that was also induced by NDAT was also anticipated, given the existing evidence that NDAT is pro-apoptotic [14, 23]. The agent appears to affect both the intrinsic and extrinsic pathways of apoptosis.

The reduction in mitotic figures in tumors harvested from NDAT-treated animals is primarily a function of loss of cell viability. However, the drug is known to downregulate from

Fig. 6 Effect of 10 days of daily s.c. NDAT (1 mg/kg) treatment on U87MG glioblastoma xenografts. Data were collected from four animals per group and two tumors per animal, $n = 8$. *Error bars* represent ±SEM and statistical significance is compared to control, **$p < 0.001$. Quantitative representation of **a** histologic estimates of tumor area and **b** average number of mitotic figures/field examined
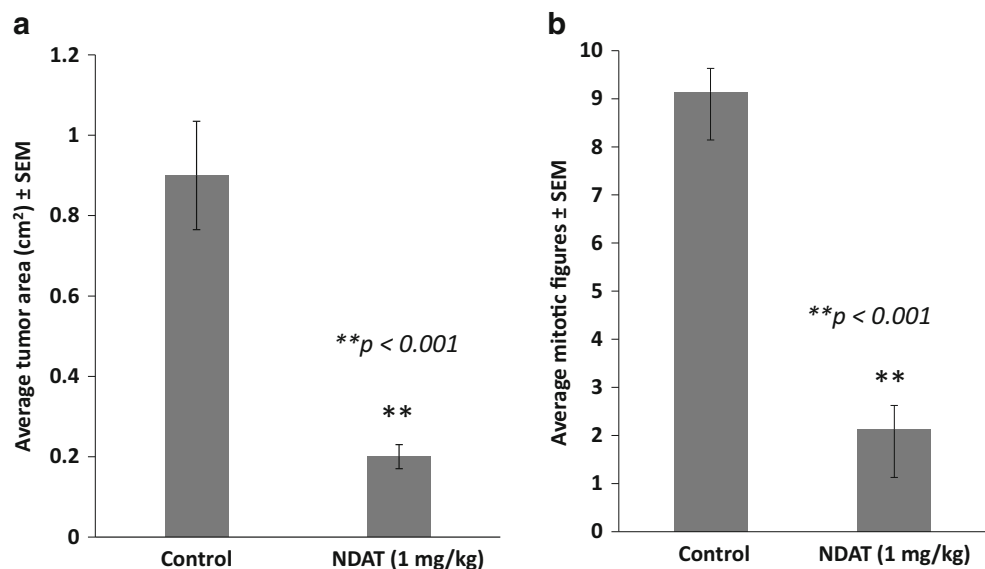
has not been examined in xenografts. The radiosensitization action of NDAT involves inhibition of repair of double-stranded DNA breaks in the tumor cell.

Finally, the PD-1 (programmed death-1)/PD-L1 (PD-ligand 1) immune checkpoint is affected by physiological concentrations of T_4, in that the hormone stimulates expression in a variety of cell lines of the *PD-L1* gene [50]. NDAT blocks this effect. This checkpoint is a focus of interest in immunotherapy of GBM [34].

What is apparent from the present studies is that NDAT has a panel of important anticancer and anti-angiogenic actions on glioblastoma xenografts. These effects are nongenomically induced at a cell surface target expressed generously by cancer cells and dividing endothelial cells. The agent is not cytotoxic and limitation of its actions to tumor and blood vessel cells explains a favorable side effect profile in preclinical studies. That is, histologic examination of organs such as the brain, heart, liver, and kidney in rodents exposed to high-dose NDAT for weeks has shown no abnormalities (S.A. Mousa, S. Sell, unpublished observations). We would also point out that the use of anti-angiogenic agents in GBM clinical management increases the risk of intratumoral hemorrhage [51, 52]. Despite the multifactorial anti-angiogenic properties of Nanotetrac, no hemorrhages occurred in the xenografts of Nanotetrac-treated animals in the present study.

A limitation of the current work is that it was carried out on xenografts of a single, widely used human glioblastoma cell line. On the other hand, we have previously shown that rat C6 and F98 glioma cell lines and mouse GL261 glioma cells proliferate in response to T_4 and that this hormonal action on these cell lines is blocked by tetrac [12]. Further, human glioblastoma clinically responds to withdrawal of thyroid hormone [11, 53]. These observations are consistent with the NDAT observations we report in the current paper. The current studies were conducted on subcutaneous xenografts. We have compared the uptake of Cy5-labeled Nanotetrac in short-term (hours) by orthotopic and subcutaneous xenografts of U87-luc cells and have confirmed that tumoral uptake across the blood-brain barrier and in subcutaneous lesions is comparable (T. Sudha, D.J. Bharali, S.A. Mousa, unpublished observations).

Compliance with Ethical Standards All animal studies were conducted at the animal facility of the Veteran Affairs Medical Center, Albany, NY, in accordance with and approved by institutional guidelines for humane animal treatment and according to the current guidelines.

Conflict of Interest Co-authors Davis and Mousa are stockholders in NanoPharmaceuticals LLC that is commercially developing NDAT (Nanotetrac, Nano-diamino-tetrac) and Davis is an officer of the company. All remaining authors have no conflicts to declare.

References

1. Omuro A, DeAngelis LM (2013) Glioblastoma and other malignant gliomas: a clinical review. JAMA 310(17):1842–1850. doi:10.1001/jama.2013.280319

2. Mrugala MM (2013) Advances and challenges in the treatment of glioblastoma: a clinician's perspective. Discov Med 15(83):221–230

3. Cloughesy TF, Cavenee WK, Mischel PS (2014) Glioblastoma: from molecular pathology to targeted treatment. Annu Rev Pathol 9:1–25. doi:10.1146/annurev-pathol-011110-130324

4. Ramirez YP, Weatherbee JL, Wheelhouse RT, Ross AH (2013) Glioblastoma multiforme therapy and mechanisms of resistance. Pharmaceuticals (Basel) 6(12):1475–1506. doi:10.3390/ph6121475

5. Alexander BM, Ligon KL, Wen PY (2013) Enhancing radiation therapy for patients with glioblastoma. Expert Rev Anticancer Ther 13(5):569–581. doi:10.1586/era.13.44

6. Chaichana KL, Cabrera-Aldana EE, Jusue-Torres I, Wijesekera O, Olivi A, Rahman M, Quinones-Hinojosa A (2014) When gross total resection of a glioblastoma is possible, how much resection should be achieved? World Neurosurg 82(1–2):e257–e265. doi:10.1016/j.wneu.2014.01.019

7. Rahmathulla G, Hovey EJ, Hashemi-Sadraei N, Ahluwalia MS (2013) Bevacizumab in high-grade gliomas: a review of its uses, toxicity assessment, and future treatment challenges. Onco Targets Ther 6:371–389. doi:10.2147/OTT.S38628

8. Mohme M, Neidert MC, Regli L, Weller M, Martin R (2014) Immunological challenges for peptide-based immunotherapy in glioblastoma. Cancer Treat Rev 40(2):248–258. doi:10.1016/j.ctrv.2013.08.008

9. Tivnan A, McDonald KL (2013) Current progress for the use of miRNAs in glioblastoma treatment. Mol Neurobiol 48(3):757–768. doi:10.1007/s12035-013-8464-0

10. Yin AA, Cheng JX, Zhang X, Liu BL (2013) The treatment of glioblastomas: a systematic update on clinical phase III trials. Crit Rev Oncol Hematol 87(3):265–282. doi:10.1016/j.critrevonc.2013.01.007

11. Hercbergs AA, Goyal LK, Suh JH, Lee S, Reddy CA, Cohen BH, Stevens GH, Reddy SK, Peereboom DM, Elson PJ, Gupta MK, Barnett GH (2003) Propylthiouracil-induced chemical hypothyroidism with high-dose tamoxifen prolongs survival in recurrent high grade glioma: a phase I/II study. Anticancer Res 23(1B):617–626

12. Davis FB, Tang HY, Shih A, Keating T, Lansing L, Hercbergs A, Fenstermaker RA, Mousa A, Mousa SA, Davis PJ, Lin HY (2006) Acting via a cell surface receptor, thyroid hormone is a growth factor for glioma cells. Cancer Res 66(14):7270–7275. doi:10.1158/0008-5472.CAN-05-4365

13. Bergh JJ, Lin HY, Lansing L, Mohamed SN, Davis FB, Mousa S, Davis PJ (2005) Integrin $\alpha v\beta 3$ contains a cell surface receptor site for thyroid hormone that is linked to activation of mitogen-activated protein kinase and induction of angiogenesis. Endocrinology 146(7):2864–2871. doi:10.1210/en.2005-0102

14. Davis PJ, Davis FB, Mousa SA, Luidens MK, Lin HY (2011) Membrane receptor for thyroid hormone: physiologic and

pharmacologic implications. Annu Rev Pharmacol Toxicol 51:99–115. doi:10.1146/annurev-pharmtox-010510-100512

15. Lin HY, Tang HY, Keating T, Wu YH, Shih A, Hammond D, Sun M, Hercbergs A, Davis FB, Davis PJ (2008) Resveratrol is pro-apoptotic and thyroid hormone is anti-apoptotic in glioma cells: both actions are integrin and ERK mediated. Carcinogenesis 29(1):62–69. doi:10.1093/carcin/bgm239

16. Lin HY, Sun M, Tang HY, Lin C, Luidens MK, Mousa SA, Incerpi S, Drusano GL, Davis FB, Davis PJ (2009) L-thyroxine vs. 3,5,3′-triiodo-l-thyronine and cell proliferation: activation of mitogen-activated protein kinase and phosphatidylinositol 3-kinase. Am J Physiol Cell Physiol 296(5):C980–C991. doi:10.1152/ajpcell.00305.2008

17. Mousa SA, Yalcin M, Bharali DJ, Meng R, Tang HY, Lin HY, Davis FB, Davis PJ (2012) Tetraiodothyroacetic acid and its nano-formulation inhibit thyroid hormone stimulation of non-small cell lung cancer cells in vitro and its growth in xenografts. Lung Cancer 76(1):39–45. doi:10.1016/j.lungcan.2011.10.003

18. Yalcin M, Bharali DJ, Dyskin E, Dier E, Lansing L, Mousa SS, Davis FB, Davis PJ, Mousa SA (2010a) Tetraiodothyroacetic acid and tetraiodothyroacetic acid nanoparticle effectively inhibit the growth of human follicular thyroid cell carcinoma. Thyroid 20(3):281–286. doi:10.1089/thy.2009.0249

19. Yalcin M, Bharali DJ, Lansing L, Dyskin E, Mousa SS, Hercbergs A, Davis FB, Davis PJ, Mousa SA (2009) Tetraidothyroacetic acid (tetrac) and tetrac nanoparticles inhibit growth of human renal cell carcinoma xenografts. Anticancer Res 29(10):3825–3831

20. Yalcin M, Dyskin E, Lansing L, Bharali DJ, Mousa SS, Bridoux A, Hercbergs AH, Lin HY, Davis FB, Glinsky GV, Glinskii A, Ma J, Davis PJ, Mousa SA (2010b) Tetraiodothyroacetic acid (tetrac) and nanoparticulate tetrac arrest growth of medullary carcinoma of the thyroid. J Clin Endocrinol Metab 95(4):1972–1980. doi:10.1210/jc.2009-1926

21. Yalcin M, Lin HY, Sudha T, Bharali DJ, Meng R, Tang HY, Davis FB, Stain SC, Davis PJ, Mousa SA (2013) Response of human pancreatic cancer cell xenografts to tetraiodothyroacetic acid nanoparticles. Horm Cancer 4(3):176–185. doi:10.1007/s12672-013-0137-y

22. Davis PJ, Sudha T, Lin HY, Mousa SA (2015) Thyroid hormone, hormone analogs, and angiogenesis. Compr Physiol 6(1):353–362. doi:10.1002/cphy.c150011

23. Davis PJ, Glinsky GV, Lin H-Y, Leith JT, Hercbergs A, Tang H-Y, Ashur-Fabian O, Incerpi S, Mousa SA (2014) Cancer cell gene expression modulated from plasma membrane integrin αvβ3 by thyroid hormone and nanoparticulate tetrac. Front Endocrinol (Lausanne) 5:240. doi:10.3389/fendo.2014.00240

24. Bharali DJ, Yalcin M, Davis PJ, Mousa SA (2013) Tetraiodothyroacetic acid-conjugated PLGA nanoparticles: a nanomedicine approach to treat drug-resistant breast cancer. Nanomedicine (Lond) 8(12):1943–1954. doi:10.2217/nnm.12.200

25. Lin HY, Landersdorfer CB, London D, Meng R, Lim CU, Lin C, Lin S, Tang HY, Brown D, Van Scoy B, Kulawy R, Queimado L, Drusano GL, Louie A, Davis FB, Mousa SA, Davis PJ (2011) Pharmacodynamic modeling of anti-cancer activity of tetraiodothyroacetic acid in a perfused cell culture system. PLoS Comput Biol 7(2):e1001073. doi:10.1371/journal.pcbi.1001073

26. Drean A, Goldwirt L, Verreault M, Canney M, Schmitt C, Guehennec J, Delattre JY, Carpentier A, Idbaih A (2016) Blood-brain barrier, cytotoxic chemotherapies and glioblastoma. Expert Rev Neurother:1–16. doi:10.1080/14737175.2016.1202761

27. Seystahl K, Wick W, Weller M (2016) Therapeutic options in re-current glioblastoma—an update. Crit Rev Oncol Hematol 99:389–408. doi:10.1016/j.critrevonc.2016.01.018

28. Venur VA, Peereboom DM, Ahluwalia MS (2015) Current medical treatment of glioblastoma. Cancer Treat Res 163:103–115. doi:10.1007/978-3-319-12048-5_7

29. Thomas AA, Omuro A (2014) Current role of anti-angiogenic strategies for glioblastoma. Curr Treat Options in Oncol 15(4):551–566. doi:10.1007/s11864-014-0308-2

30. Lieberman NA, Moyes KW, Crane CA (2016) Developing immunotherapeutic strategies to target brain tumors. Expert Rev Anticancer Ther 16(7):775–788. doi:10.1080/14737140.2016.1192470

31. Peschillo S, Caporlingua A, Diana F, Caporlingua F, Delfini R (2016) New therapeutic strategies regarding endovascular treatment of glioblastoma, the role of the blood-brain barrier and new ways to bypass it. J Neurointerv Surg 8(10):1078–1082. doi:10.1136/neurintsurg-2015-012048

32. von Neubeck C, Seidlitz A, Kitzler HH, Beuthien-Baumann B, Krause M (2015) Glioblastoma multiforme: emerging treatments and stratification markers beyond new drugs. Br J Radiol 88(1053):20150354. doi:10.1259/bjr.20150354

33. Kalkan R (2015) Glioblastoma stem cells as a new therapeutic target for glioblastoma. Clin Med Insights Oncol 9:95–103

34. Desai R, Suryadevara CM, Batich KA, Farber SH, Sanchez-Perez L, Sampson JH (2016) Emerging immunotherapies for glioblastoma. Expert Opin Emerg Drugs 21(2):133–145. doi:10.1080/14728214.2016.1186643

35. Vogelbaum MA (2007) Convection enhanced delivery for treating brain tumors and selected neurological disorders: symposium review. J Neuro-Oncol 83(1):97–109. doi:10.1007/s11060-006-9308-9

36. Vogelbaum MA, Aghi MK (2015) Convection-enhanced delivery for the treatment of glioblastoma. Neuro-Oncology 17(Suppl 2):ii3–ii8. doi:10.1093/neuonc/nou354

37. Vogelbaum MA, Iannotti CA (2012) Convection-enhanced delivery of therapeutic agents into the brain. Handb Clin Neurol 104:355–362. doi:10.1016/B978-0-444-52138-5.00023-2

38. Vogelbaum MA, Sampson JH, Kunwar S, Chang SM, Shaffrey M, Asher AL, Lang FF, Croteau D, Parker K, Grahn AY, Sherman JW, Husain SR, Puri RK (2007) Convection-enhanced delivery of cintredekin besudotox (interleukin-13-pe38qqr) followed by radiation therapy with and without temozolomide in newly diagnosed malignant gliomas: phase 1 study of final safety results. Neurosurgery 61(5):1031–1037. doi:10.1227/01.neu.0000303199.77370.9ediscussion 1037-1038

39. Dvorak HF (2015a) Tumor stroma, tumor blood vessels, and antiangiogenesis therapy. Cancer J 21(4):237–243. doi:10.1097/PPO.0000000000000124

40. Dvorak HF (2015b) Tumors: wounds that do not heal-redux. Cancer Immunol Res 3(1):1–11. doi:10.1158/2326-6066.CIR-14-0209

41. Peng L, Bu Z, Zhou Y, Ye X, Liu J, Zhao Q (2014) Hemorrhagic events in cancer patients treated with aflibercept: a meta-analysis. Tumour Biol 35(9):9419–9427. doi:10.1007/s13277-014-2189-1

42. Letarte N, Bressler LR, Villano JL (2013) Bevacizumab and central nervous system (cns) hemorrhage. Cancer Chemother Pharmacol 71(6):1561–1565. doi:10.1007/s00280-013-2155-4

43. Narita Y (2013) Drug review: safety and efficacy of bevacizumab for glioblastoma and other brain tumors. Jpn J Clin Oncol 43(6):587–595. doi:10.1093/jjco/hyt051

44. Davis PJ, Goglia F, Leonard JL (2016) Nongenomic actions of thyroid hormone. Nat Rev Endocrinol 12(2):111–121. doi:10.1038/nrendo.2015.205

45. Lin HY, Chin YT, Yang YC, Lai HY, Wang-Peng J, Liu LF, Tang HY, Davis PJ (2016a) Thyroid hormone, cancer, and apoptosis. Compr Physiol 6(3):1221–1237. doi:10.1002/cphy.c150035

46. Mousa SA, Lin HY, Tang HY, Hercbergs A, Luidens MK, Davis PJ (2014) Modulation of angiogenesis by thyroid hormone and hormone analogues: implications for cancer management. Angiogenesis 17(3):463–469. doi:10.1007/s10456-014-9418-5

47. Davis FB, Mousa SA, O'Connor L, Mohamed S, Lin HY, Cao HJ, Davis PJ (2004) Proangiogenic action of thyroid hormone is fibroblast growth factor-dependent and is initiated at the cell surface.

Circ Res 94(11):1500–1506. doi:10.1161/01.RES.0000130784.90237.4a

48. Shih A, Zhang S, Cao HJ, Tang HY, Davis FB, Davis PJ, Lin HY (2004) Disparate effects of thyroid hormone on actions of epidermal growth factor and transforming growth factor-alpha are mediated by 3′,5′-cyclic adenosine 5′-monophosphate-dependent protein kinase II. Endocrinology 145(4):1708–1717. doi:10.1210/en.2003-0742

49. Hercbergs AH, Lin HY, Davis FB, Davis PJ, Leith JT (2011) Radiosensitization and production of DNA double-strand breaks in U87MG brain tumor cells induced by tetraiodothyroacetic acid (tetrac). Cell Cycle 10(2):352–357. doi:10.4161/cc.10.2.14641

50. Lin HY, Chin YT, Nana AW, Shih YJ, Lai HY, Tang HY, Leinung M, Mousa SA, Davis PJ (2016b) Actions of l-thyroxine and nano-diamino-tetrac (nanotetrac) on PD-L1 in cancer cells. Steroids 114:59–67. doi:10.1016/j.steroids.2016.05.006

51. Fraum TJ, Kreisl TN, Sul J, Fine HA, Iwamoto FM (2011) Ischemic stroke and intracranial hemorrhage in glioma patients on antiangiogenic therapy. J Neuro-Oncol 105(2):281–289. doi:10.1007/s11060-011-0579-4

52. Mamo A, Baig A, Azam M, Rho YS, Sahebjam S, Muanza T, Owen S, Petrecca K, Guiot MC, Al-Shami J, Sharma R, Kavan P (2016) Progression pattern and adverse events with bevacizumab in glioblastoma. Curr Oncol 23(5):e468–e471. doi:10.3747/co.23.3108

53. Hercbergs A, Johnson RE, Ashur-Fabian O, Garfield DH, Davis PJ (2015) Medically induced euthyroid hypothyroxinemia may extend survival in compassionate need cancer patients: an observational study. Oncologist 20(1):72–76. doi:10.1634/theoncologist.2014-0308